J Mater Sci (2018) 53:3927–3938

Review

Recent achievements on sulfide-type solid electrolytes: crystal structures and electrochemical performance

Ze Ma[1], Huai-Guo Xue[1], and Sheng-Ping Guo[1,*]

[1] School of Chemistry and Chemical Engineering, Yangzhou University, Yangzhou 225002, Jiangsu, People's Republic of China

Received: 19 September 2017
Accepted: 14 November 2017
Published online: 27 November 2017

ABSTRACT

The all-solid-state lithium batteries using solid electrolytes are considered to be the new generation of devices for energy storage, which might be a key solution for power electric and hybrid electric vehicles in the future. This review focuses on the crystal structures and electrochemical properties of sulfide solid electrolytes. They are classified to several subgroups according to their chemical compositions, namely thiophosphates, halide thiophosphates, sulfide without phosphorus, and glassy sulfides electrolytes, which might be potential solid electrolytes in lithium batteries and may replace the currently used polymeric electrolytes for LIBs. Through discussion, this review provides an insight into future promising sulfide electrolytes.

Introduction

Energy innovation plays an important role in the reduction of carbon emission in the atmosphere and global warming. Progresses are necessary in energy storage technology for the integration of intermittent renewable energy resources on electricity markets and grids [1]. Lithium-ion batteries (LIBs) have become essential in most portable electronic products because of their high energies and power densities since they were first commercialized by Sony in the 1990s [2, 3]. It is well known that high-performance electrolyte materials have great influences on the batteries' performance. Compared with solid electrolytes, liquid electrolytes have some intrinsic risks such as explosion, flammability, and volatilization. For example, $LiBF_4$, $LiPF_6$, and $LiCF_3SO_3$ dissolved in organic solvents such as ethylene carbonate, propylene carbonate, polyethylene oxide, and dimethyl carbonate, are flammable and have poor electrochemical stability and a limited temperature range of operation [4–8]. Because of the intrinsic solid character, solid electrolytes are much safer than liquid ones. The main advantages of solid electrolytes are that they do not corrode, combust, leak, or cause internal shorting like their liquid counterparts [9]. Although several technological issues still need to be addressed, including the development of a processing technology using sheeting and multiple stacking, the all-solid-state batteries can be considered a future category of electrochemical devices [10, 11]. Moreover, solid electrolytes are inert toward metallic Li and act as a separator, helping resist to dendrite growth. Solid electrolytes need to possess a relatively high ionic conductivity ($\sigma > 10^{-3}$ S/cm). However,

Address correspondence to E-mail: spguo@yzu.edu.cn

https://doi.org/10.1007/s10853-017-1827-6

most existing solid electrolytes have a long way to achieve this goal [12, 13].

Compared with liquid and polymer ones (around 1×10^{-2} S/cm), solid electrolytes (SEs) have relatively much lower ionic conductivities (10^{-5}–10^{-3} S/cm) under room temperature. This shortcoming restricts the practical utilization of solid batteries in view of the less effective electrode–electrolyte interface and insufficient understanding of interfacial reaction mechanism [14, 15]. Sulfide-type SEs also have their own drawbacks should be solved, such as poor thermal stabilities, easily to be moisture absorption, expensive raw materials like Li_2S, and easy to react with lithium metal generated impedance layer, which makes the solid-state batteries gradually deteriorated during cycling. These disadvantages restrict the further applications of sulfide-type SEs. In recent years, to alleviate or overcome the above shortcomings, various doping, coating, and nanostructure modifications of sulfide SEs have been reported [4, 5]. SEs need to possess the following characteristics for their large-scale applications in Li batteries in the future [16, 17]:

1. High ionic conductivity to reduce the resistance polarization effects in a solid battery at room temperature;
2. Interfacial impedance and grain boundary resistance, negligible electronic conductivity;
3. Wide electrochemical stability window;
4. Chemical stability in the presence of electrodes, especially metallic Li anodes;
5. Matching thermal expansion coefficients with both electrodes;
6. More easily polarizable;
7. Low cost, high throughput, easy synthesis, and environmental benignity.

SEs for LIBs should be Li-ion conductors, which require high ionic conductivities at room temperature and low activation energies (E_a) for their use over a broad range of operating temperatures [18, 19]. Table 1 shows known inorganic solid electrolytes. Compared with oxide-type ones, sulfide-type electrolytes have smaller electronegativity and binding force to Li^+ ion. On the other hand, the bigger ionic radius of S compared with O induces a larger ion channels in the structure and benefits to ionic mobility [20, 21]. Compared with other types of inorganic solid electrolytes, sulfide ones have the highest ionic conductivities in the present, which might be 10^{-4}–10^{-3} S/cm and have high electrochemical stabilities up to ~ 5 V versus Li^+ ion at room temperature [22–24].

In this review, known sulfide-type solid electrolytes are summarized and classified into several parts according to their chemical compositions, including thiophosphates, halide thiophosphates, sulfides without phosphorus, and glassy sulfides electrolytes (Fig. 1). We try to provide researchers new insights into exploring ionic conductors with high conductivities and wide electrochemical windows.

Table 1 Classification of inorganic solid electrolytes

(ISEs)	Classification		Compound{σ_{Li+}(S/cm)}
Oxide solid electrolytes	Amorphous		xLi_2O–$(1-x)SiO_2$
			xLi_2O–$(1-x)BO_2$
	Crystalline	Lithium Superionic Conductors	$Li_{14}Zn(GeO_4)_4$ {0.13 S/cm at 300 °C}
		Sodium Superionic Conductors	$Li_{1+x}Al_xGe_{2-x}(PO_4)_3$
			$Li_{1.3}Al_{0.3}Ti_{1.7}(PO_4)_3$ {3.00×10^{-3}}
		Perovskite	$Li_{3x}La_{2/3-x}TiO_3$
			$Li_{0.34}La_{0.51}TiO_{2.94}$ {1.00×10^{-3}}
		Garnet	$Li_7La_3Zr_2O_{12}$
			$Li_{6.55}La_3Zr_2Ga_{0.15-0.3}O_{12}$ {1.30×10^{-3}}
Sulfide solid electrolytes	Amorphous		xLi_2S–$(1-x)P_2S_5$
	Crystalline		$Li_{10}GeP_2S_{12}$ {1.20×10^{-2} S/cm}
Nitride solid electrolytes	Amorphous	LiPON	LiPON
	Crystalline	Lithium nitride	Li_3N

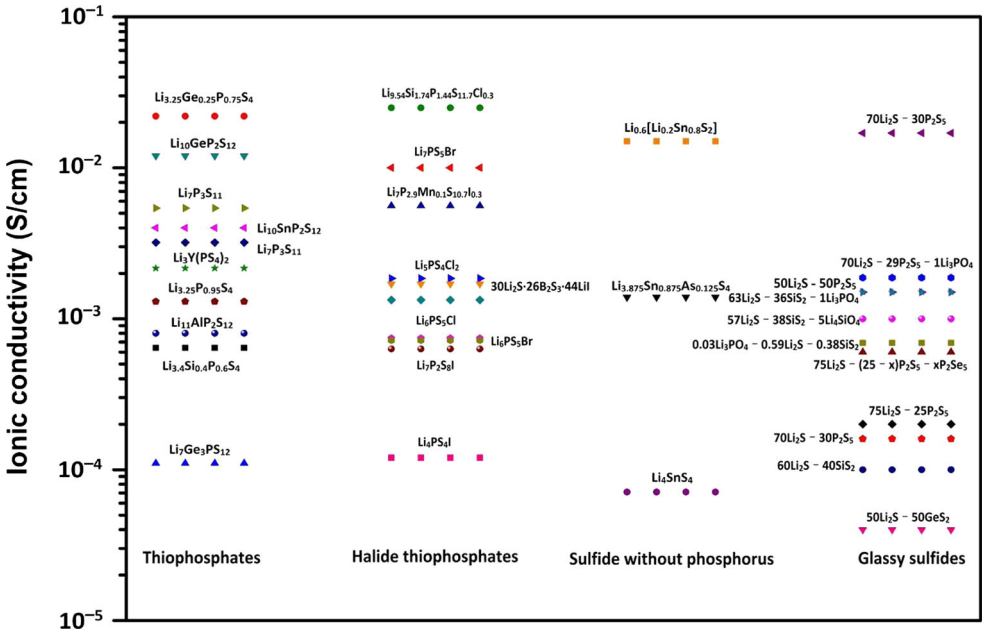

Figure 1 Reported ionic conductivities of solid electrolyte materials at room temperature, including thiophosphates, halide thiophosphates, sulfides without phosphorus, and glassy sulfides. Only materials with conductivities above 1×10^{-5} S/cm included.

Sulfide-type solid electrolytes

According to their chemical compositions, sulfide-type solid electrolytes are classified into thiophosphates, halide thiophosphates, sulfides without phosphorus, and glassy sulfide electrolytes. Thiophosphates, halide thiophosphates, and sulfide without phosphorus are all crystalline. Glassy sulfide electrolytes contain glass–ceramic and glass ones.

Thiophosphates

To date, many thiophosphates have been extensively investigated as solid electrolytes for batteries (Table 2). According to their chemical compositions, they can be classified into the following subgroups.

Li–P–S

Tachez et al. discovered a new sulfide solid electrolyte Li_3PS_4 with a conductivity of 3×10^{-7} S/cm and an activation energy of 0.46 eV, which is a pioneering work on crystalline sulfide-type SEs containing P. The electrochemical window of Li_3PS_4 ranges from 0.6 to 3.7 V [35]. Later, many investigations on Li_3PS_4 and $Li_7P_3S_{11}$ were carried out [38–41]. Phuc et al. [38] prepared plate-like $3 \times 0.5 \times 0.1 \sim 0.2\ \mu m^3$ Li_3PS_4 (Fig. 2). The ionic conductivity of the prepared Li_3PS_4 was about 2.0×10^{-4} S/cm at room temperature. This work pointed out that the usage of nanosized-solid electrolyte could result in a high loading of active materials, which then enhanced the specific energy of the all-solid-state cells.

In 2007, Yamane et al. [33] obtained $Li_7P_3S_{11}$ with a high conductivity of 3.2×10^{-3} S/cm and an activation energy of 12 kJ/mol. It crystallizes in the triclinic space group $P\bar{1}$. Its structure can be described as a PS_4 tetrahedron- and P_2S_7 di-tetrahedron-built framework, and Li^+ ions locate at the polyhedral cavities (Fig. 3). Highly crystalline $Li_7P_3S_{11}$ was obtained by a precipitation reaction from the glasses P_2S_3–P_2S_5 [32]. The as-prepared $Li_7P_3S_{11}$ has a higher conductivity than of that of $Li_7P_3S_{11}$ prepared using Al_2O_3 media [35]. In 2015, Huang et al. reported Li_3PO_4-doped $Li_7P_3S_{11}$ glass–ceramic electrolytes with the highest total conductivity of 1.87×10^{-3} S/cm at 25 °C and the lowest activation energy of 18 kJ/mol. The triclinic $Li_7P_3S_{11}$ prepared from $70Li_2S$ to $30P_2S_5$ (mol%) exhibits the highest Li^+ ion conductivity among the $xLi_2S - (100 - x)P_2S_5$ (mol%) systems. Compared with Li_3PS_4, $Li_7P_3S_{11}$ seems have higher conductivity and lower activation energy. Much smaller size and more symmetrical structure may improve the electrolyte's conductivity [42].

Li–X–P–S

In 2013, Wang et al. obtained thio-LISICON $Li_{3.25}Ge_{0.25}P_{0.75}S_4$ using a low-temperature solution

Table 2 Ionic conductivities of thiophosphate SEs

Compound	σ_{Li}^{+} (S/cm)	E_a	Space group	Ref.
$Li_{3.4}Si_{0.4}P_{0.6}S_4$	6.40×10^{-4} (RT[a])	–	–	[25]
$Li_{3.25}Ge_{0.25}P_{0.75}S_4$	2.20×10^{-2} (298 K)	–	–	[26]
$Li_{3.25}Ge_{0.25}P_{0.75}S_4$	2.2×10^{-3} (298 K)	–	–	[27]
$Li_{3.25}Ge_{0.25}P_{0.75}S_4$	1.82×10^{-4} (303 K)	0.42 (20 kJ/mol)	–	[28]
$Li_7Ge_3PS_{12}$	1.1×10^{-4} (298 K)	25 kJ/mol	–	[29]
$Li_{10}GeP_2S_{12}$	1.2×10^{-2} (300 K)	0.2 eV	$P4_2/nmc$	[30]
$Li_{10}SnP_2S_{12}$	4×10^{-3} (300 K)	–	$P4_2/nmc$	[31]
$Li_7P_3S_{11}$	5.4×10^{-3} (298 K)	–	$P\bar{1}$	[32]
$Li_7P_3S_{11}$	3.2×10^{-3} (RT)	12 kJ/mol	$P\bar{1}$	[33]
$Li_{3.25}P_{0.95}S_4$	1.3×10^{-3} (298 K)	–	–	[34]
Li_3PS_4	3×10^{-7} (298 K)	–	–	[35]
$Li_3Y(PS_4)_2$	2.16×10^{-3} (300 K)	0.278 eV	$C2/c$	[36]
$Li_{11}AlP_2S_{12}$	8.02×10^{-4} (298 K)	–	–	[37]

[a]*RT* room temperature

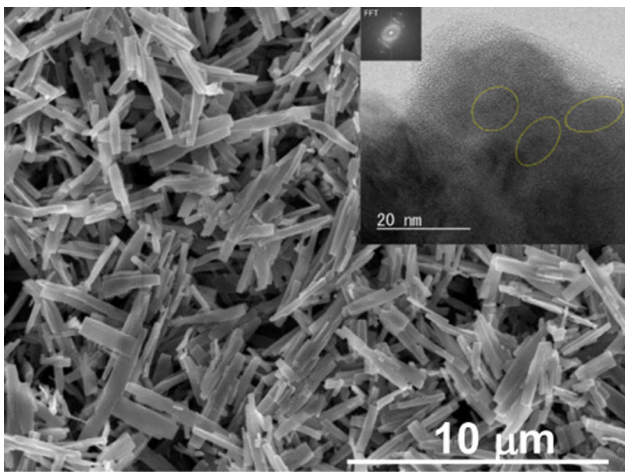

Figure 2 SEM and HR-TEM (small inset) images of Li_3PS_4 [38]. @ 2017, Springer.

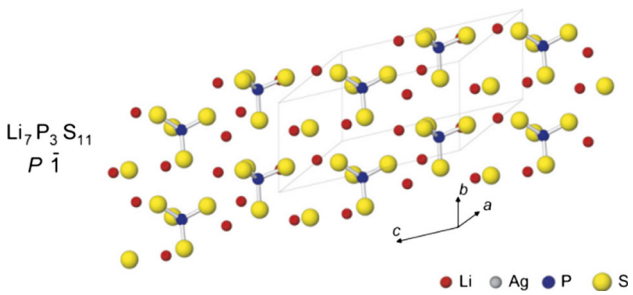

Figure 3 Crystal structure of $Li_7P_3S_{11}$ [33]. @ 2007, Elsevier.

method. The $Li_{3.25}Ge_{0.25}P_{0.75}S_4$ film shows a Li^+ ion conductivity of 1.82×10^{-4} S/cm at 30 °C and an activation energy of 0.42 eV [28]. Inoue et al. synthesized $Li_7Ge_3PS_{12}$ by slow cooling from the ternary Li_2S–GeS_2–P_2S_5 system, which adopts a cubic argyrodite-type structure (Fig. 5b), and exhibits a high ionic conductivity of 1.1×10^{-4} S/cm at 25 °C and an activation energy of 25 kJ/mol [29]. Kamaya et al. reported a Li^+ superionic conductor $Li_{10}GeP_2S_{12}$ (LGPS), which has a new 3D framework structure consisting of $(Ge_{0.5}P_{0.5})S_4$, PS_4 and LiS_4 tetrahedra, and LiS_6 octahedra [30]. It exhibits an extremely high Li^+ ionic conductivity of 12 mS/cm at room temperature (Fig. 4). This new solid battery electrolyte has many advantages in terms of device fabrication (facile shaping, patterning, and integration), stability (non-volatile), safety (non-explosive), and excellent electrochemical properties [high conductivity and wide electrochemical window (0.0–5.0 V)]. Later,

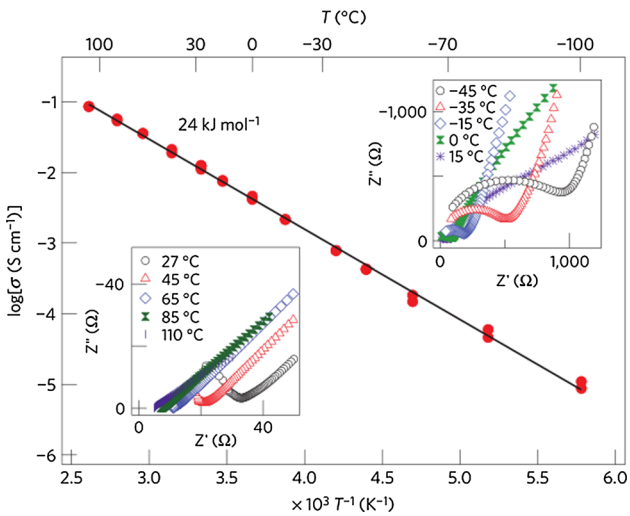

Figure 4 Impedance plots of the conductivity data from low to high temperatures and Arrhenius conductivity plots of $Li_{10}GeP_2S_{12}$ [43]. © 2011, Nature Publish Group.

LGPS intrigued much interest. Mo et al. found a metastable phase LGPS from the calculated phase diagram in 2012 [30]. They also found that LGPS was not stable against reduction by Li at a low voltage or extraction of Li^+ ions with decomposition at a high voltage. The ionic conduction in LGPS happens in three dimensions, rather than in one dimension. In 2014, Liang et al. studied two distinct Li^+ ion diffusion processes in the tetragonal LGPS along 1D tunnel ($E_a = 0.16$ eV) and in a plane perpendicular to the 1D tunnel ($E_a = 0.26$ eV), respectively, which were separately verified by Li and P multiple solid-state NMR methods, Wang et al. studied the influences of the anion-host matrixes on the ionic conductivities of Li^+ ion conductors. A new descriptor emerges from their discoveries: anion sublattices with bcc-like frameworks are superior for Li-ion diffusion as it leads to a lower activation barrier than in other close packed frameworks. The bcc anion framework allows the Li^+ ions to migrate within a network of interconnected tetrahedral sites possessing equivalent energies. This feature is also found in recently synthesized superionic Li-ion conductors, such as $Li_{10}GeP_2S_{12}$ and $Li_7P_3S_{11}$ [30]. These new conclusions can be employed to explore fast ion conductors with improved properties [32].

Encouraged by the success of LGPS, many scientists also paid their attention to LXPS (X = Sn, Al, Y, Si et al.). $Li_{10}SnP_2S_{12}$ crystallizes in the tetragonal space group $P4_2/nmc$ [31]. It has a total conductivity of 4 mS/cm at 27 °C. The replacement of Ge by Sn can largely reduce the cost. Zhou et al. synthesized $Li_{11}AlP_2S_{12}$ for the first time by sintering at 500 °C in 2016. $Li_{11}AlP_2S_{12}$ has a conductivity of 8.02×10^{-4} S/cm at 25 °C, a low E_a of 25.4 kJ/mol, and a wide electrochemical voltage window of above 5.0 V (vs. Li^+/Li), indicating its promising application in solid-state LIBs [37, 44–46]. Zhu et al. found Li−M−P−S (M: non-redox-active element Ge, Al, Y et al.) [47, 48]. The phase and electrochemical stability of $Li_3Y(PS_4)_2$ (Fig. 5) is expected to be better than current state-of-the-art Li^+ superionic conductors [36].

In general, thiophosphate SEs have been widely researched. People focused on improving electrolytes' conductivity and reducing active energy. Some effective methods can reach this goal, such as controlling electrolytes' size and structure, mingling some non-redox-active element, and optimizing synthesis methods.

Halide thiophosphates (argyrodite)

Apart from ionic conductivity (Table 3), the electrochemical stability window for solid electrolyte is also one of the most important criteria for battery applications. Most nonmetal electrolytes with phosphorus have the electrochemical stability up to ~ 5 V versus Li at room temperature. In 2012, Boulineau et al. reported Li-argyrodite Li_6PS_5X (X = Cl, Br, I). The chemical formulae of Li_6PS_5X (X = Cl, Br, I) are based on a substitution pattern from the corresponding Ag and Cu compounds, in which S atoms is replaced by X atoms, and S and X atoms ordered on separate crystallographic sites [53].

Li_6PS_5Cl obtained via ball milling has a conductivity of 1.33×10^{-3} S/cm with an electrochemical stability up to 7 V versus Li^+ [52]. It crystallizes in the cubic space group $F\,\bar{4}\,3\,m$ (Fig. 6). The first preliminary results showed that the $In/Li_6PS_5Cl/LiCoO_2$ solid electrolyte battery has encouraging electrochemical performance. In 2016, Kato et al. reported Li^+ superionic conductor $Li_{9.54}Si_{1.74}P_{1.44}S_{11.7}Cl_{0.3}$ with an extra high conductivity of 25 mS/cm, as well as high stability (~ 0 V vs. Li metal for $Li_{9.6}P_3S_{12}$). A fabricated all-solid-state cell based on this lithium conductor was found to have very small internal resistance, especially at 100 °C.

Rangasamy et al. obtained $Li_7P_2S_8I$ by the reaction of β-Li_3PS_4 and LiI, which shows an electrochemical stability up to 10 V versus Li/Li^+ (Fig. 7) [58]. The oxidation instability of I is subverted via its incorporation into the structure. The inclusion of I also creates stability with the metallic Li anode while simultaneously enhancing the interfacial kinetics and ionic conductivity. Low-temperature membrane processability enables facile fabrication of dense membranes, making this conductor suitable for industrial application.

Sulfide electrolytes with halogen elements may have higher electrochemical windows. Current investigations are underway to identify the crystal structures and mechanisms of Li-ion conduction in the newly formed phases along with polymeric reinforcement for flexible solid electrolyte membranes. This opens new avenues for the development of inherently safe all-solid Li batteries.

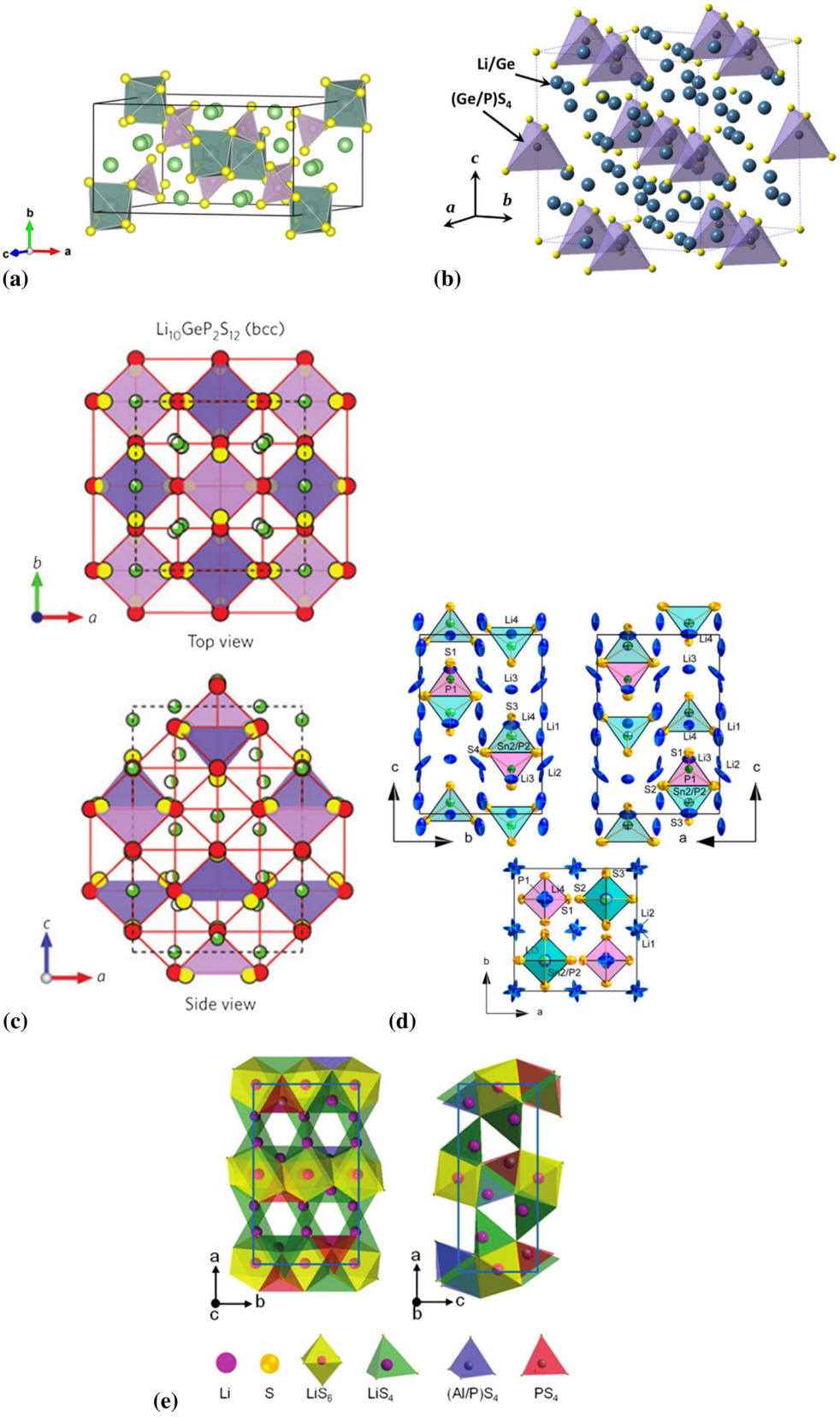

Figure 5 Crystal structures of **a** $Li_3Y(PS_4)_2$ [36], $Li_7Ge_3PS_{12}$ (yellow: S; blue: Li/Ge; purple tetrahedron: **b** $(Ge/P)S_4$) [29], **c** $Li_{10}GeP_2S_{12}$ [49], **d** $Li_{10}SnP_2S_{12}$ [31], and **e** $Li_{11}AlP_2S_{12}$ [37]. @ 2017, American Chemical Society; 2017, Elsevier; 2015, Nature Publish Group; 2013, American Chemical Society; 2016, Royal Society of Chemistry.

Table 3 Ionic conductivities of halide thiophosphates

Compound	σ_{Li+} (S/cm)	E_a (eV)	Space group	Ref.
Li_7PS_5Br	10^{-2}	0.2	–	[50]
$Li_5PS_4Cl_2$	1.85×10^{-3} (300 K)	0.304	*C*2 *mm*	[2]
Li_6PS_5Cl	1.33×10^{-3}	29–39 kJ/mol	$F\bar{4}3m$	[51]
Li_6PS_5Cl	7.4×10^{-4} (RT)	11 kJ/mol	$F\bar{4}3m$	[52]
Li_6PS_5Br	7.2×10^{-4} (RT)	16 kJ/mol	$F\bar{4}3m$	[53]
Li_6PS_5I	4.6×10^{-7} (RT)	24 kJ/mol	$F\bar{4}3m$	[53]
$Li_7P_2S_8I$	6.3×10^{-4} (RT)	–	*Pnma*	[53]
Li_4PS_4I	1.2×10^{-4}	0.43	*P*4/*nmm*	[54]
$Li_{9.54}Si_{1.74}P_{1.44}S_{11.7}Cl_{0.3}$	2.5×10^{-2}	–	–	[55]
$Li_7P_{2.9}Mn_{0.1}S_{10.7}I_{0.3}$	5.6×10^{-3} (RT)	–	$P\bar{1}$	[56]

RT room temperature

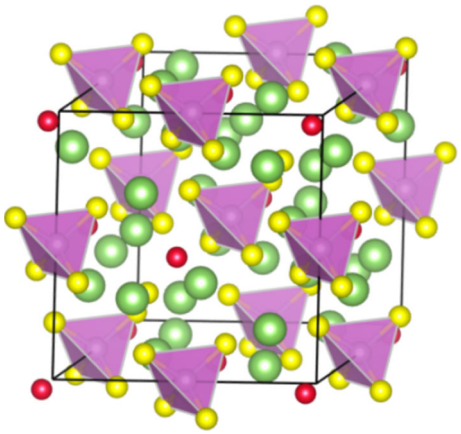

Figure 6 Crystal structure of Li_6PS_5Cl determined from DFT calculations. Li^+: green, Cl^-: red, S^{2-}: yellow, and $(PS_4)^{3-}$ tetrahedron: purple [57]. @ 2016, American Chemical Society.

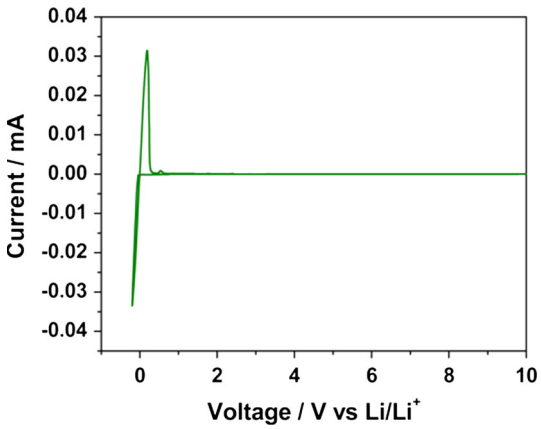

Figure 7 Cyclic–voltammogram curve for a $Li/Li_7P_2S_8I/Pt$ cell at 1 mV/s, showing that $Li_7P_2S_8I$ is stable up to 10 V versus Li/Li^+ [51]. @ 2015, American Chemical Society.

Nonmetal sulfide SEs without phosphorus

The ionic conductivities of SEs without phosphorus are simply summarized in Table 4. Among them, isostructural $Li_{0.6}[Li_{0.2}Sn_{0.8}S_2]$ and $Li[Li_{0.33}Sn_{0.67}S_2]$ crystallize in the monoclinic space group *C*2/*c*, belonging to the Na_2IrO_3 structure-type, an ordered variant of the layered α-$NaFeO_2$ structure. The structural difference between Na_2IrO_3 and α-$NaFeO_2$ is that the latter contains alternating layers of Na and Fe fourfold-coordinated with O atoms featuring a mixed Na/Ir layer ordered in a honeycomb framework [60]. $Li_{0.6}[Li_{0.2}Sn_{0.8}S_2]$ shows a conductivity of 1.5×10^{-2} S/cm. The activation energy of $Li[Li_{0.33}Sn_{0.67}S_2]$ is 0.17 eV, which is comparable to values for the currently best LISICONs such as $Li_{10}GeP_2S_{12}$ (0.21 eV) and $Li_{11}Si_2PS_{12}$ (0.19 eV).

Li_4SnS_4 crystallizes in the orthorhombic space group *Pnma* with Z = 4 (Fig. 8). Its structure features isolated SnS_4 tetrahedra. It shows a very promising Li^+ ion conductivity of 7×10^{-5} S/cm at 20 °C and 3×10^{-3} S/cm at 100 °C, which is exceptionally high for a ternary compound. An activation energy for Li^+ ion transport measured via impedance spectroscopy (0.41 eV) correlates reasonably well with the values (0.29–0.33 eV) deduced from ionic mobility studies by Li solid-state NMR spectroscopy [61]. Li_2GeS_3 crystallizes in the orthorhombic space group *Pnma*, and with conductivity of 9.7×10^{-9} S/cm [62].

The matrix of $Li_{4-x}S_{n-x}As_xS_4$ ($x = 0$–0.250) is Li_4SnS_4 (space group *Pnma*). $Li_{3.875}Sn_{0.875}As_{0.125}S_4$ has a high ionic conductivity of 1.39 mS/cm at 25 °C. The lowest activation energy was observed in the composition of $Li_{3.833}Sn_{0.833}As_{0.166}S_4$ that had the highest ionic conductivity among the $Li_{4-x}Sn_{1-x}As_xS_4$

Table 4 Ionic conductivities of SEs without phosphorus

Compound	σ_{Li+} (S/cm)	E_a (eV)	Space group	Ref.
$Li_{0.6}[Li_{0.2}Sn_{0.8}S_2]$	1.5×10^{-2}	–	–	[59]
Li_4SnS_4	7.1×10^{-5} (298 K)	–	*Pnma*	[60]
Li_2GeS_3	9.7×10^{-9} (298 K)	–	*Pnma*	[61]
$Li_{3.875}Sn_{0.875}As_{0.125}S_4$	1.39×10^{-3} (298 K)	–	–	[62]
$Li_{3.833}Sn_{0.833}As_{0.166}S_4$	1.39×10^{-3} (298 K)	0.21 eV/20 kJ/mol	–	[63]

RT room temperature

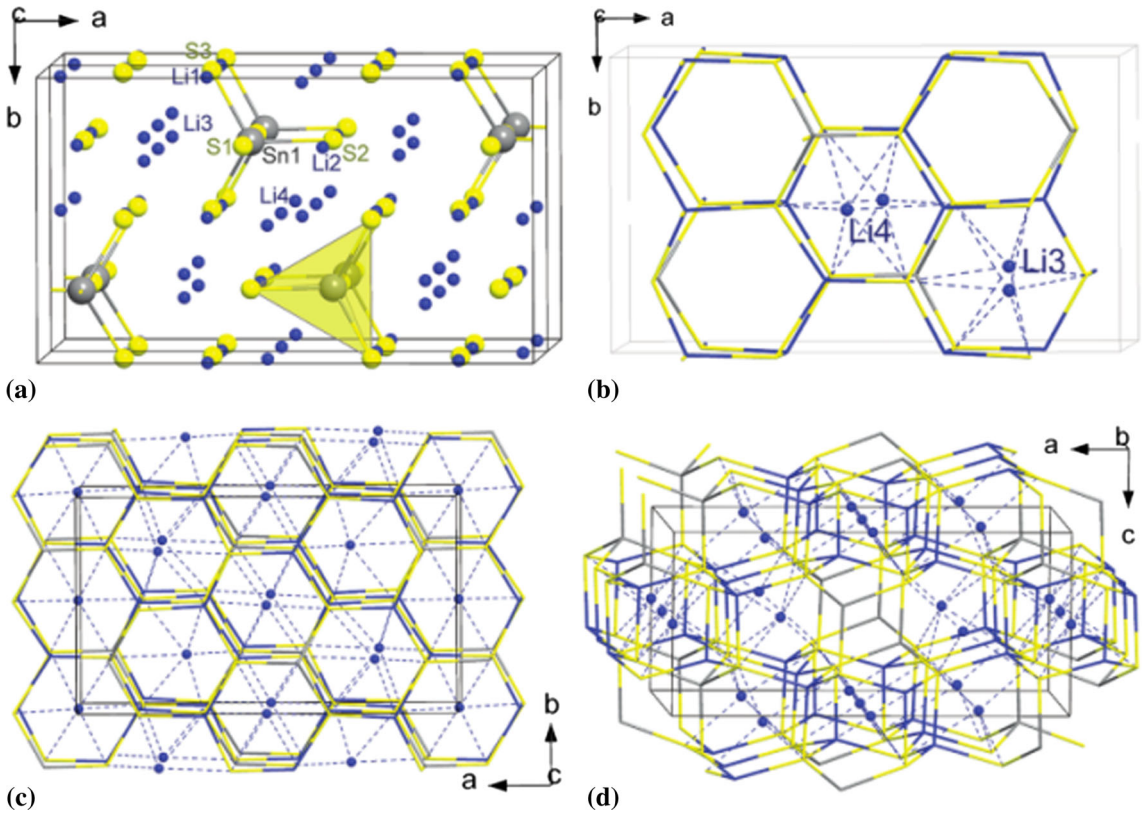

Figure 8 Crystal structure of Li_4SnS_4 [58]. © 2012, American Chemical Society.

($x = 0$–0.250) compounds. The activation energy was as low as 0.21 eV as compared to other well-known solid electrolytes. All XRD patterns show that the structure of $Li_{4-x}Sn_{1-x}As_xS_4$ is the Li_4SnS_4-type (space group *Pnma*) [63].

Glass electrolytes

Ionic conductivities of glass and glass–ceramic SEs are summarized in Table 5. It can be noticed that there are many chemical compositions can be tuned among these materials.

Glass–ceramic

Glass–ceramic electrolytes can be prepared by the crystallization of precursor glasses. The crystallization usually would decrease the ionic conductivities, but the precipitation of a superionic conducting crystal from a precursor glass can enhance the ionic conductivity. The grain boundaries around crystal domains in glass–ceramics are filled with amorphous phases. Thus, glass–ceramic electrolytes usually have lower grain boundary resistances than polycrystalline systems [66]. A heat-treated Li_2S–P_2S_5 glass–ceramic conductor has a high ionic conductivity of 1.7×10^{-2} S/cm [63]. The $75Li_2S$–$25P_2S_5$ (mol%)

Table 5 Ionic conductivities of glass and glass–ceramic SEs

Compound	σ_{Li}^{+} (S/cm)	E_a (eV)	Structure	Ref.
$70Li_2S–30P_2S_5$	1.7×10^{-2} (RT)	17 kJ/mol	Glass–ceramic	[63]
$Li_2S–P_2S_5$	1.5×10^{-3}(RT)	0.35	Glass–ceramic	[64]
$75Li_2S–25P_2S_5$	2×10^{-4} (RT)	34 kJ/mol	Amorphous	[65]
$70Li_2S–30P_2S_5$	1.6×10^{-4} (298 K)	12 kJ/mol	Glass–ceramic	[66]
$70Li_2S–29P_2S_5–1Li_3PO_4$	1.87×10^{-3} (298 K)	18 kJ/mol	Glass–ceramic	[67]
$63Li_2S–36SiS_2–1Li_3PO_4$	1.5×10^{-3} (298 K)	0.3	Glass	[57]
$57Li_2S–38SiS_2–5Li_4SiO_4$	10^{-3} (298 K)	–	Glass	[57]
$0.03Li_3PO_4–0.59Li_2S–0.38SiS_2$	6.9×10^{-4} (RT)	–	Glass	[68]
$60Li_2S–40SiS_2$ (mol%)	10^{-4} (RT)	–	Glass	[69]
$75Li_2S–(25–x)P_2S_5–xP_2Se_5$	6×10^{-4} (RT)	–	Amorphous and crystalline	[70]
$50Li_2S–50GeS_2$	4.0×10^{-5} (298 K)	–	Glass	[57]

RT room temperature

amorphous powders obtained by mechanical milling have a conductivity of 2×10^{-4} S/cm at room temperature and an activation energy of 34 kJ/mol [65]. Glass–ceramic electrolyte has a high ionic conductivity at room temperature and a negligible electronic conductivity. Advantages of the glass–ceramic SEs over the crystalline ones might include their relatively lower heat treatment temperatures.

Glass

The glassy electrolytes have attracted much attention mainly due to their several advantages over the crystalline materials: isotropic ionic conduction, no grain boundary resistance, ease to be fabricated into film, a wide range of compositions, etc. [71].

Generally, Li^+ ion conducting glasses can be divided into oxides and sulfides. For most of the oxide ones, their conductivities at room temperature are too low to be practical for high-energy batteries, normally on the order of 10^{-6}–10^{-8} S/cm [16], while for sulfide ones, the conductivities of 10^{-3}–10^{-5} S/cm at room temperature can be achieved in view of high polarizability of S^{2-} ions, such as $Li_2S–SiS_2$ and $Li_2S–P_2S_5$ [71].

Glassy sulfide-type ion conductive materials from $Li_2S–P_2S_5$ with doped LiI have been investigated extensively. Kennedy and Zhang reported a class of $Li_2S–SiS_2$ glasses doped with LiX with an ionic conductivity higher than 10^{-4} S/cm [69]. Numerous glass sulfide electrolytes based on $xLi_2S–(1-x)P_2S_5$ and $(x)Li_2S–(1-x)SiS_2$ have been synthesized, mostly using mechanical milling technique. Shin et al. prepared amorphous and crystalline $Li_2S–(25-x)P_2S_{5-x}P_2Se_5$, and the crystalline one has a conductivity of about 6×10^{-4} S/cm.

Kennedy firstly synthesized the $Li_2S–SiS_2$ SE using a melting-quench method in 1986 [70]. It had an ion conductivity from 10^{-6} to 10^{-3} S/cm. The composition of $0.6(0.4SiS_2–0.6Li_2S)–0.4LiI$ showed the highest conductivity of 1.8×10^{-3} S/cm and an activation energy of 0.28 eV. Since then, $Li_2S–SiS_2$-based glass electrolytes have been widely investigated aiming to improve the ion conductivities and electrochemical stabilities. Besides, high-energy ball-milled amorphous $Li_2S–SiS_2$ showed a conductivity of 1.5×10^{-4} S/cm, and $Li_2S–SiS_2$ system doped with Li_3PO_4 had a conductivity of 6.9×10^{-4} S/cm with high electrochemical reduction stability [69]. The utilization of combining sulfide and oxide anions and the precipitation of superionic metastable crystals from glasses are effective ways to improve the Li^+ conductivity of glass–based solid electrolytes [71]. Activation energy of $63Li_2S·36SiS_2·1Li_3PO_4$ was 0.30 eV, and conductivity (298 K) was 1.6×10^{-3} S/cm [56]. The conductivity of a mechanochemically prepared $60Li_2S·40SiS_2$ (mol%) was around 10^{-4} S/cm at room temperature [69]. The conductivities of the $Li_2S–P_2S_5$ system could be further improved with the formation of crystalline phases by glass crystallization.

Conclusion and outlook

In summary, solid electrolytes are potential materials for batteries because of their safety and high performance. Therefore, sulfide-type solid electrolytes have higher ionic conductivities and wide electrochemical

stability windows than other solid electrolytes. We discussed several types of sulfide electrolytes and make conclusions as follows:

1. Nonmetal electrolytes have been widely studied, which can obtain high ionic conductivity via controlling size and crystal structure.
2. Halide electrolytes have been reported with very wide electrochemical stability window (~ 10 V vs. Li).
3. Glassy electrolytes have several advantages over the crystalline materials: isotropic ionic conduction, no grain boundary resistance, ease to be fabricated into film, a wide range of compositions, etc.
4. Sulfide halide-type SEs containing phosphorus may become a potential material with higher ionic conductivity.
5. The mechanical properties (particularly the malleability and the ductility) of the SE and the electrode materials have a great impact on the contact condition of electrolyte and electrode materials. To improve the solid–solid contact between the electrolyte and the electrode materials, it is necessary to improve the mechanical properties of the SE.
6. A body-centered cubic (bcc) anion sublattice allows the lowest activation barrier and highest ionic conductivity. The bcc anion framework allows the Li ions to migrate within a network of interconnected tetrahedral sites possessing equivalent energies.
7. One of the future studies should be focused on elucidation of the phase relationships in the low- and high-temperature phases of materials.

Acknowledgements

We gratefully acknowledge the financial support by National Natural Science Foundation of China (Grant Nos. 21673203 and 21771159), the Higher Education Science Foundation of Jiangsu Province (No. 15KJB150031), State Key Laboratory of Structural Chemistry Fund (No. 20150009), the Priority Academic Program Development of Jiangsu Higher Education Institutions, and the Qing Lan project.

References

[1] Hueso KB, Armand M, Rojo T (2013) High temperature sodium batteries: status, challenges and future trends. Energy Environ Sci 6:734–749

[2] Armand M, Tarascon JM (2008) Building better batteries. Nature 451:652–657

[3] He X, Zhu Y, Mo Y (2017) Origin of fast ion diffusion in super-ionic conductors. Nature Commun 8:15893. https://doi.org/10.1038/ncomms15893

[4] Bachman JC, Muy S, Grimaud A, Chang HH, Pour N, Lux SF, Paschos O, Maglia F, Lupart S, Lamp P, Giordano L, Shao-Horn Y (2015) Inorganic solid-state electrolytes for lithium batteries: mechanisms and properties governing ion conduction. Chem Rev 116:140–162

[5] Thangadurai V, Narayanan S, Pinzaru D (2014) Garnet-type solid-state fast Li ion conductors for Li batteries: critical review. Chem Soc Rev 43:4714–4727

[6] Naqash S, Ma QL, Tietz F, Guillon O (2017) $Na_3Zr_2(SiO_4)_2(PO_4)$ prepared by a solution-assisted solid state reaction. Solid State Ion 302:83–91

[7] Kim H, Ding Y, Kohl PA (2012) LiSICON–ionic liquid electrolyte for lithium ion battery. J Power Sources 198:281–286

[8] Teng ZY, Lv HY, Wang CY, Xue HG, Pang H, Wang GX (2017) Bandgap engineering of ultrathin graphene-like carbon nitride nanosheets with controllable oxygenous functionalization. Carbon 113:63–75

[9] Baek SW, Honma I, Kim J, Rangappa D (2017) Solidified inorganic-organic hybrid electrolyte for all solid state flexible lithium battery. J Power Sources 343:22–29

[10] Raj R, Wolfenstine J (2017) Current limit diagrams for dendrite formation in solid-state electrolytes for Li-ion batteries. J Power Sources 343:119–126

[11] Yan Y, Li B, Guo W, Pang H, Xue HG (2016) Vanadium based materials as electrode materials for high performance supercapacitors. J Power Sources 329:148–169

[12] Gao J, Zhao YS, Shi SQ, Li H (2016) Lithium–ion transport in inorganic solid state electrolyte. Chin Phys B 25:018211. https://doi.org/10.1088/1674-1056/25/1/018211

[13] Li F, Kitaura H, Zhou H (2013) The pursuit of rechargeable solid-state Li–air batteries. Energy Environ Sci 6:2302–2311

[14] Anantharamulu N, Koteswara Rao K, Rambabu G, Kumar BV, Radha V, Vithal M (2011) A wide-ranging review on Nasicon type materials. J Mater Sci 46:2821–2837. https://doi.org/10.1007/s10853-011-5302-5

[15] Wu BB, Wang SY, Evans WJ, Deng DZ, Yang JH, Xiao J (2016) Interfacial behaviors between lithium ion conductors and electrode materials in various battery systems. J Mater Chem A 4:15266–15280

[16] Chen RJ, Qu WJ, Guo X, Li L, Wu F (2016) The pursuit of solid-state electrolytes for lithium batteries: from comprehensive insight to emerging horizons. Mater Horiz 3(6):487–516

[17] Lin Z, Liang C (2015) Lithium–sulfur batteries: from liquid to solid cells. J Mater Chem A 3:936–958

[18] Goodenough JB, Park KS (2013) The Li-ion rechargeable battery: a perspective. J Am Chem Soc 135:1167–1176

[19] Varzi A, Raccichini R, Passerini S, Scrosati B (2016) Challenges and prospects of the role of solid electrolytes in the revitalization of lithium metal batteries. J Mater Chem A 4:17251–17259

[20] Adnan S, Mohamed NS (2014) Effects of Sn substitution on the properties of Li_4SiO_4 ceramic electrolyte. Solid State Ion 262:559–562

[21] Li XR, Xue HG, Pang H (2017) Facile synthesis and shape evolution of well-defined phosphotungstic acid potassium nanocrystals as a highly efficient visible-light-driven photocatalyst. Nanoscale 9:216–222

[22] Park M, Zhang XC, Chung M, Less GB, Sastry AM (2010) A review of conduction phenomena in Li-ion batteries. J Power Sources 195:7904–7929

[23] Lu XC, Xia GG, Lemmon JP, Yang ZG (2010) Advanced materials for sodium-beta alumina batteries: status, challenges and perspectives. J Power Sources 195:2431–2442

[24] Knauth P (2009) Inorganic solid Li ion conductors: an overview. Solid State Ion 180:911–916

[25] Murayama M, Kanno R, Irie M, Ito S, Hata T, Sonoyama N, Kawamoto Y (2002) Synthesis of new lithium ionic conductor thio-LISICON—lithium silicon sulfides system. J Solid State Chem 168:140–148

[26] Kobayashi T, Inada T, Sonoyama N, Yamada A, Kanno R (2004) All solid-state batteries using super ionic conductor, thio-LISICON–electrode/electrolyte interfacial design. In: MRS online proceedings library archive 835

[27] Kanno R, Murayama M (2001) Lithium ionic conductor thio-LISICON: the $Li_2SGeS_2P_2S_5$ system. J Electrochem Soc 148:A742–A746

[28] Wang YM, Liu ZQ, Zhu XL, Tang YF, Huang FQ (2013) Highly lithium-ion conductive thio-LISICON thin film processed by low-temperature solution method. J Power Sources 224:225–229

[29] Inoue Y, Suzuki K, Matsui N, Hirayama M, Kanno R (2017) Synthesis and structure of novel lithium-ion conductor $Li_7Ge_3PS_{12}$. J Solid State Chem 246:334–340

[30] Wang ZQ, Wu MS, Liu G, Lei XL, Xu B, Ouyang CY (2014) Elastic properties of new solid state electrolyte material $Li_{10}GeP_2S_{12}$: a study from first-principles calculations. Int J Electrochem Sci 9:562–568

[31] Bron P, Johansson S, Zick K, aufderGuenne JS, Dehnen S, Roling B (2013) $Li_{10}SnP_2S_{12}$: an affordable lithium superionic conductor. J Am Chem Soc 135:15694–15697

[32] Kowada Y, Tatsumisago M, Minami T, Adachi H (2008) Electronic state of sulfide-based lithium ion conducting glasses. J Non Cryst Solids 354:360–364

[33] Yamane H, Shibata M, Shimane Y, Junke T, Seino Y, Adams S, Minami K, Hayashi A, Tatsumisago M (2007) Crystal structure of a superionic conductor, $Li_7P_3S_{11}$. Solid State Ion 178:1163–1167

[34] Hayashi A, Tatsumisago M (2012) Recent development of bulk-type solid-state rechargeable lithium batteries with sulfide glass-ceramic electrolytes. Electron Mater Lett 8(2):199–207

[35] Tachez M, Malugani J, Mercier R, Robert G (1984) Ionic conductivity of and phase transition in lithium thiophosphate Li_3PS_4. Solid State Ion 14:181–185

[36] Zhu ZY, Chu IH, Ong SP (2017) $Li_3Y(PS_4)_2$ and $Li_5PS_4Cl_2$: new lithium superionic conductors predicted from silver thiophosphates using efficiently tiered ab initio molecular dynamics simulations. Chem Mater 29:2474–2484

[37] Zhou PF, Wang JB, Cheng FY, Li FJ, Chen J (2016) A solid lithium superionic conductor $Li_{11}AlP_2S_{12}$ with a thio-LISICON analogous structure. Chem Commun 52:6091–6094

[38] Phuc NHH, Morikawa K, Mitsuhiro T, Muto H, Matsuda A (2017) Synthesis of plate-like Li3PS4 solid electrolyte via liquid-phase shaking for all-solid-state lithium batteries. Ionics 23(8):2061–2067

[39] Baek SW, Honma I, Kim J, Rangappa D (2017) Solidified inorganic-organic hybrid electrolyte for all solid state flexible lithium battery. J Power Sources 343:22–29

[40] Liu ZC, Fu WJ, Payzant EA, Yu X, Wu ZL, Dudney NJ, Kiggans J, Hong KL, Rondinone AJ, Liang CD (2013) Anomalous high ionic conductivity of nanoporous β-Li_3PS_4. J Am Chem Soc 135:975–978

[41] Teragawa S, Aso K, Tadanaga K, Hayashi A, Tatsumisago M (2014) Liquid-phase synthesis of a Li_3PS_4 solid electrolyte using N-methylformamide for all-solid-state lithium batteries. J Mater Chem A 2:5095–5099

[42] Wu QH, Chen M, Chen KY, Wang SS, Wang CJ, Diao GW (2016) Fe_3O_4-based core/shell nanocomposites for high-performance electrochemical supercapacitors. J Mater Sci 51:1572–1580. https://doi.org/10.1007/s10853-015-9480-4

[43] Noriaki K, Kenji H, Yuichiro Y, Masaaki H, Ryoji K, Masao Y, Takashi K, Kato Yuki, Shigenori H, Koji K, Akio M (2011) A lithium superionic conductor. Nat Mater 10(9):682–686

[44] Guo SP, Ma Z, Li JC, Xue HG (2017) First investigation of the electrochemical performance of γ-$LiFeO_2$ micro-cubes as promising anode material for lithium-ion batteries. J Mater

Sci 52:1469–1476. https://doi.org/10.1007/s10853-016-0441-3

[45] Guo SP, Ma Z, Li JC, Xue HG (2017) Facile preparation and promising lithium storage ability of α-$LiFeO_2$/porous carbon nanocomposite. J Alloys Compd 711:8–14

[46] Guo SP, Li JC, Ma Z, Chi Y, Xue HG (2017) A facile method to prepare FeS/porous carbon composite as advanced anode material for lithium-ion batteries. J Mater Sci 52:2345–2355. https://doi.org/10.1007/s10853-016-0527-y

[47] Mariappan CR, Yada C, Rosciano F, Roling B (2011) Correlation between micro-structural properties and ionic conductivity of $Li_{1.5}Al_{0.5}Ge_{1.5}(PO_4)_3$ ceramics. J Power Sources 196:6456–6464

[48] Zhao PC, Wen YH, Cheng J, Cao GP, Jin ZQ, Ming H, Xu Y, Zhu XY (2017) A novel method for preparation of high dense tetragonal $Li_7La_3Zr_2O_{12}$. J Power Sources 344:56–61

[49] Wang Y, William DR, Shyue PO, Lincoln JM, Jae CK, Yifei M, Gerbrand C (2015) Design principles for solid-state lithium superionic conductors. Nat Mater 14(10):1026–1031

[50] Epp V, Gun O, Deiseroth HJ, Wilkening M (2013) Highly mobile ions: low-temperature NMR directly probes extremely fast Li^+ hopping in argyrodite-type Li_6PS_5Br. J Phys Chem Lett 4:2118–2123

[51] Boulineau S, Courty M, Tarascon JM, Viallet V (2012) Mechanochemical synthesis of Li-argyrodite Li_6PS_5X (X = Cl, Br, I) as sulfur-based solid electrolytes for all solid state batteries application. Solid State Ion 221:1–5

[52] Rayavarapu P, Sharma N, Peterson V, Adams S (2012) Variation in structure and Li^+-ion migration in argyrodite-type Li_6PS_5X (X=Cl, Br, I) solid electrolytes. J Solid State Electrochem 16:1807–1813

[53] Rangasamy E, Liu ZC, Gobet M, Pilar K, Sahu G, Zhou W, Wu H, Greenbaum S, Liang CD (2015) An iodide-based $Li_7P_2S_8I$ superionic conductor. J Am Chem Soc 137:1384–1387

[54] Sedlmaier SJ, Indris S, Dietrich C, Yavuz M, Dräger C, Seggern FV, Sommer H, Janek J (2017) Li_4PS_4I: a Li^+ superionic conductor synthesized by a solvent-based soft chemistry approach. Chem Mater 29:1830–1835

[55] Kato Y, Hori S, Saito T, Suzuki K, Hirayama M, Mitsui A, Yonemura M, Iba H, Kanno R (2016) High-power all-solid-state batteries using sulfide superionic conductors. Nature Energy 1:16030. https://doi.org/10.1038/nenergy.2016.30

[56] Xu RC, Xia XH, Li SH, Zhang SZ, Wang XL, Tu JP (2017) All-solid-state lithium–sulfur batteries based on a newly designed $Li_7P_{2.9}Mn_{0.1}S_{10.7}I_{0.3}$ superionic conductor. J Mater Chem A 5:6310–6317

[57] Deng Z, Zhu ZY, Chu IH, Shyue PO (2016) Data-driven first-principles methods for the study and design of alkali superionic conductors. Chem Mater 29(1):281–288

[58] Rangasamy E, Liu ZC, Gobet M, Pilar K, Sahu G, Zhou W, Wu H, Greenbaum S, Liang CD (2015) An iodide-based $Li_7P_2S_8I$ superionic conductor. J Am Chem Soc 137:1384–1387

[59] Holzmann T, Schoop LM, Ali MN, Moudrakovski I, Gregori G, Maier J, Cava RJ, Lotsch BV (2016) $Li_{0.6}[Li_{0.2}Sn_{0.8}S_2]$–a layered lithium superionic conductor. Energy Environ Sci 9:2578–2585

[60] Kaib T, Haddadpour S, Kapitein M, Bron P, Schröder C, Eckert H, Roling B, Dehnen S (2012) New lithium chalcogenidotetrelates, LiChT: synthesis and characterization of the Li^+-conducting tetralithium ortho-sulfidostannate Li_4SnS_4. Chem Mater 24:2211–2219

[61] Kanno R, Hata T, Kawamoto Y, Irie M (2000) Synthesis of a new lithium ionic conductor, thio-LISICON–lithium germanium sulfide system. Solid State Ion 130:97–104

[62] Sahu G, Lin Z, Li J, Liu Z, Dudney N, Liang C (2014) Air-stable, high-conduction solid electrolytes of arsenic-substituted Li_4SnS_4. Energy Environ Sci 7:1053–1058

[63] Seino Y, Ota T, Takada K, Hayashi A, Tatsumisago M (2014) A sulphides lithium super ion conductor is superior to liquid ion conductors for use in rechargeable batteries. Energy Environ Sci 7:627–631

[64] Liu ZQ, Tang YF, Wang YM, Huang FQ (2014) High performance Li_2S–P_2S_5 solid electrolyte induced by selenide. J Power Sources 260:264–267

[65] Hayashi A, Hama S, Morimoto H, Tatsumisago M, Minami T (2001) Preparation of Li_2S–P_2S_5 amorphous solid electrolytes by mechanical milling. J Am Ceram Soc 84:477–479

[66] Tatsumisago M, Hayashi A (2008) All-solid-state lithium secondary, batteries using sulfide-based glass ceramic electrolytes. Funct Mater Lett 1:31–36

[67] Huang BX, Yao XY, Huang Z, Guan YB, Jin Y, Xu XX (2015) Li_3PO_4-doped $Li_7P_3S_{11}$ glass-ceramic electrolytes with enhanced lithium ion conductivities and application in all-solid-state batteries. J Power Sources 284:206–211

[68] Kondo S, Takada K (1992) New lithium ion conductors based on Li_2S–SiS_2 system. Solid State Ion 53–56:1183–1186

[69] Morimoto H, Yamashita H, Tatsumisago M, Mechanochemical TM (1999) Mechanochemical synthesis of new amorphous materials of $60Li_2S$ $40SiS_2$ with high lithium ion conductivity. J Am Ceram Soc 82:1352–1354

[70] Kim J, Yoon Y, Eom M, Shin D (2012) Characterization of amorphous and crystalline Li_2S–P_2S_5–P_2Se_5 solid electrolytes for all-solid-state lithium ion batteries. Solid State Ion 225:626–630

[71] Cao C, Li ZB, Wang XL, Zhao BX, Han WQ (2014) Recent advances in inorganic solid electrolytes for lithium batteries. Frontiers Energy Res 2:25. https://doi.org/10.3389/fenrg.2014.00025